Journal of Energy Storage 27 (2020) 101057

Contents lists available at ScienceDirect

Journal of Energy Storage

journal homepage: www.elsevier.com/locate/est

An IGDT-based risk-involved optimal bidding strategy for hydrogen storage-based intelligent parking lot of electric vehicles

Jun Liu[a], Chong Chen[b], Zhenling Liu[c], Kittisak Jermsittiparsert[d,*], Noradin Ghadimi[e]

[a] School of Economics and Management, Zhengzhou University of Light Industry, Zhengzhou, 450001, China
[b] School of business and administration, Henan University of Economics and Law, Zhengzhou, 450001, China
[c] School of Management, Henan University of Technology, Zhengzhou 450001, China
[d] Social Research Institute, Chulalongkorn University, Bangkok, Thailand
[e] Young Researchers and Elite Club, Islamic Azad University, Ardabil Branch, Ardabil, Iran

ARTICLE INFO

Keywords:
Social welfare of owners of electric vehicles
Intelligent parking lot
Optimal bidding curve
Power price policy
IGDT technique
Energy management and business

ABSTRACT

In a near future, electric vehicles (EVs) will constitute considerable part of transportation systems due to their important aspects such as being environment friendly. To manage high number of EVs, developing hydrogen storage-based intelligent parking lots (IPLs) can help power system operators to overcome caused problems by high penetration of EVs. In this work, a new method is applied to get optimal management of IPLs in an uncertain environment and provide optimal bidding curves to take part in power market. The main purpose of this work is to get optimal bidding curves with considering power price uncertainty and optimal operation of IPLs. To model uncertainty of power price in the power market and develop optimal bidding curve, the opportunity, deterministic and robustness functions of the information gap decision theory (IGDT) technique has been developed. Obtained results has been presented in three strategies namely risk-taker, risk-neutral, and risk-averse corresponding to opportunity, deterministic, and robustness functions of the IGDT technique. In order to demonstrate the effects of demand response program (DRP), each strategy is optimized with and without DRP cases. The mixed-integer non-linear programming model is used to formulate the proposed problem which is solved using the GAMS optimization software under DICOPT solver.

1. Introduction

By increasing number of electric vehicles day by day, the power system operators should prepare themselves to deal with this new phenomenon. Based on prediction of the research institute of electric power system, at the end of 2050, plug-in hybrid vehicles will constitute more than sixty percent of vehicles in US [1]. Not only EVs are not simple energy consumers, also they are active players in the power system imposing many challenges on optimal system operation due to their high uncertainty level [2]. To deal with raised problems by the EVs, intelligent parking lots (IPLs) can be considered as a feasible and reliable solution [3]. Intelligent parking lots act as a charging point for high number of EVs which eases managing numerous EVs dispersed in the different part of the distribution system [4]. Therefore optimal operation of IPLs should be well-studied [5].

1.1. Literature review

In the literature, many worthy works has been published in field of optimal operation and management of the IPLs in different situation which will be briefly reviewed in the following. By introducing new concepts, exchanged energy between the EVs and upstream network is investigated in [6]. Optimal discharging and charging management of EVs is surveyed using the game theory method in [7]. Considering residential and commercial places, scheduling of the EV is pursued during day and night by utilizing two-stage approximate dynamic programming framework in [8]. In a personal parking lot, scheduling of EVs' discharge is investigated by taking parking patterns of EVs into account in [9]. In a reserve and joint energy markets optimal charging and discharging of EVs are studied considering requirements of EV owner in [10]. Considering uncertain driving patterns of EV, optimal sitting of IPL of electric vehicles in the distribution system is carried out using a probabilistic method in [11]. To get online demand coordination between distribution system and EVs, a fuzzy system is proposed in [12].

* Correspondence author.
E-mail address: kittisak.j@chula.ac.th (K. Jermsittiparsert).

https://doi.org/10.1016/j.est.2019.101057
Received 24 August 2019; Received in revised form 27 October 2019; Accepted 31 October 2019
Available online 09 November 2019

In [13], to estimate discharge capacity of IPL, which is equipped with roof top PV, a mathematical model is proposed. As energy storage systems, batteries of parked EVs in the IPL are considered in [14] to take part in reserve market. With the goal of power loss and operating cost minimization of the system, and increment system reliability, optimal IPL placement is investigated in [15]. To get discharge/charge modes of EVs in large capacities, a conventional IPL is turned to IPL in [16]. Different parameters of EVs are considered in [17] to raise the sale of energy stored of EVs. In [18], optimal energy scheduling of huge number of EVs in an urban IPL is investigated. A stochastic discharge and charge scheduling of EV in the IPL is carried out in [19]. In [20], an efficient stochastic based dynamic programming method is introduced to optimally charge an EV. A bi-objective framework is developed in [21] to minimize the emission and operational cost using the ε-constraint method. To pinpoint the optimal location and size of IPL considering the reliability of distribution system, multi-objective problem for an IPL is provided in [22-24]. A deterministic model to analyze behavior of EVs is presented in [25] using the Markov-chain technique to optimize the discharge and charge processes.

1.2. Novelty and contribution

Up until now, many worthy works are carried out on planning and operation of IPL. But, as far as we know, process of participating in power market in the present of power price uncertainty has not been considered in the previous works. Therefore, the main aim of the present paper is to provide optimal bidding strategy to submit to the power market by the operator of the IPL. To do so, IGDT technique is used to develop a mechanism to construct optimal bidding-curve for each hour. To get better analysis of the operation of the system, obtained results has been presented in risk-taker, risk-neutral, and risk-averse strategies corresponding to opportunity, deterministic, and robustness functions of the IGDT technique, each of which, has been solved with and without DRP. The novelty and contributions of this work are clearly provided below.

1 Optimal bidding strategy for hydrogen storage-based intelligent parking lot of electric vehicles is obtained.
2 IGDT technique is proposed to develop a mechanism to construct optimal bidding strategy.
3 Risk-taker, risk-neutral, and risk-averse strategies are analyzed via the proposed IGDT technique.
4 The effects of demand response program in each strategy are investigated.

1.3. Paper organization

The rest of this paper is categorized as follows: Deterministic formulation of the problem is provided in Section 2. The IGDT method and its implementation on the problem are detailed in Section 3. The obtained results are discussed in Section 4. Finally, the conclusion of this work is provided in Section 5.

2. Deterministic formulation

The under system study is illustrated in Fig. 1 [18] which is consisted of RESs including WTs and PVs, MTs, HSS, and load. In the developed case study, the DRPs are considered as virtual generation units to reduce operating cost by smoothing out the load curve. To exchange energy with the upstream-grid and satisfy the required load demand, it is assumed that the system operates in grid-connected mode. Upstream grid price uncertainty is modeled using the proposed IGDT technique. In other words, IGDT technique is applied to create optimal bidding curve for each hour which has been submitted to the power market by the operator of the IPL. Furthermore, the risk-taker, risk-neutral, and risk-averse strategies corresponding to opportunity, deterministic, and robustness functions of the IGDT technique are obtained considering with and without DRP.

In order to get optimal operation strategy, the operator of the IPL needs to get required information including the initial SOC of EV, power limits of discharge/charge modes, EV's expected SOC at departure, and elapsed-time of battery-life as soon as EVs enter to the IPL. By considering mentioned data, the system operator can developed optimal charging and discharging strategies to minimize its operating cost. In should be noted that to optimize performance of IPL, a central controller as an interface between the upstream network and IPL is required.

2.1. Objective function

Minimizing the cost function of the IPL, which is presented in Eq. (1), is the main aim of the IPL operator considering power exchange between IPL and upstream-grid.

$$OBJ = \sum_{t=1}^{T}\left[\left(P_{UG}^{t}\times\pi_{UG}^{t}+\sum_{j=1}^{G}(C_{LDG}^{j,t}+SC_{LDG}^{j,t}+SHC_{LDG}^{j,t})+\sum_{i=1}^{N}(-P_{Ch,EV}^{i,t}\times\pi_{Ch,EV}^{i}+P_{Dch,EV}^{i,t}\times\pi_{Dch,EV}^{i})\right)\times\Delta t\right] \tag{1}$$

where,
Indices

i, tIndicators of EV and time
jIndicators of DG
Parameters
π_{UG}^{t}Upstream network price
$\pi_{Ch,Ev}^{i}$, $\pi_{Dch,Ev}^{i}$EV's charging and discharging price in the IPL
ΔtSampling period to count available EVs in the IPL
Decision variables
OBJObjective function
P_{UG}^{t}IPL's purchased power from the upstream network
$C_{LDG}^{j,t}$DG's operation cost
$SC_{LDG}^{j,t}$DG's start-up cost in each time
$SHC_{LDG}^{j,t}$DG's shut-down cost in each time
$P_{Ch,Ev}^{i,t}$, $P_{Dch,Ev}^{i,t}$EV's charged/discharged power

The first term of Eq. (1) refers to the cost of power procurement from the upstream network. The operating and start-up costs of the MTs are modeled by the second term of the objective function. Finally, the third term models discharging and charging costs of the parked EVs in the IPL. It should be noted that as the operator of IPL gets benefit from EVs' owners through charging their vehicles, charging cost of EVs is considered as a negative term.

2.2. Operating constraints of IPLs

To guarantee safe performance of the IPL, following constraints should be taken into account.

$$P_{Ch,EV}^{i,t}\le P_{Ch,\max}^{i}\times W_{ch}^{i,t}\times M^{i,t} \tag{2}$$

$$P_{Dch,EV}^{i,t}\le P_{Dch,\max}^{i}\times W_{Dch}^{i,t}\times M^{i,t} \tag{3}$$

$$W_{ch}^{i,t}+W_{Dch}^{i,t}\le M^{i,t} \tag{4}$$

$$\sum_{t=t_a^i}^{t_d^i} W_{ch}^{i,t}+W_{Dch}^{i,t}\le N_{\max} \tag{5}$$

$$SOC^{i,t}=SOC^{i,t-1}+P_{Ch,EV}^{i,t}\times\eta_{G2V}-P_{Dch,EV}^{i,t}/\eta_{V2G} \tag{6}$$

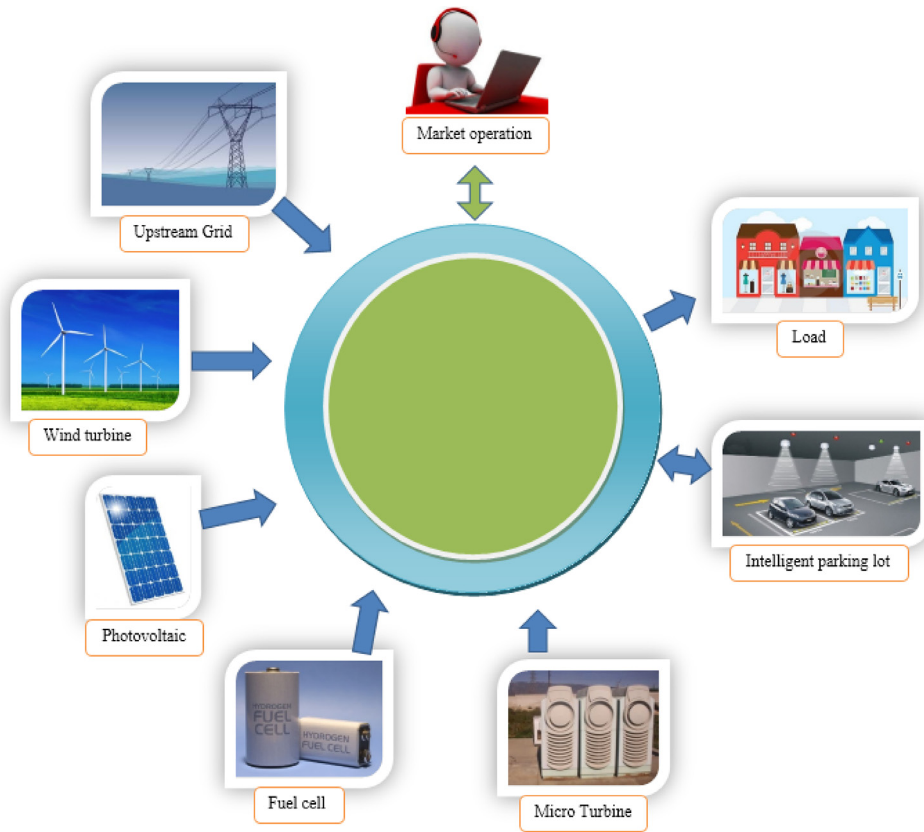

Fig. 1. An IGDT-based risk-involved the proposed model for IPL [18].

$$SOC^{i}_{\min} \le SOC^{i,t} \le SOC^{i}_{\max} \tag{7}$$

$$-\Delta SOC^{i}_{\max} \le SOC^{i,t} - SOC^{i,t-1} \le \Delta SOC^{i}_{\max} \tag{8}$$

$$SOC^{i,t}_{\text{Departure}} \ge SOC^{i}_{\max} \tag{9}$$

$$SOC^{i,t} \ge SOC^{i,t}_{Arrival} \tag{10}$$

where,

Parameters

$P^{i}_{Ch,\max}$, $P^{i}_{Dch,\max}$ Maximum limits of EV's charged and discharged power
$M^{i,\,t}$ Binary parameter; whether the EVs are in the parking lot or not
t^{i}_{a}, t^{i}_{d} Approximate arrival/departure time of EVs to/from the IPL
η_{G2V}, η_{V2G} EV's charging/discharging efficiency
$SOC^{i}_{\max}$, $SOC^{i}_{\min}$ Maximum and minimum SOC of EVs
$\Delta SOC^{i}_{\max}$ Maximum discharge/charge rate of EV
$SOC^{i,t}_{Arrival}$ The initial SOC of EV when is arrived to IPL
$N_{\max}$ Switching limit between the discharge/charge states
Decision variables
$W^{i,t}_{ch}$, $W^{i,t}_{Dch}$ Binary variable for determining charging and discharging modes
$SOC^{i,\,t}$ EV's SOC
$SOC^{i,t}_{Departure}$ EV's SOC at departure

EVs' charged power and discharged power are limited via Eqs. (2) and (3), respectively. To avoid charging and discharging of the EVs at the same time, constraint (4) is utilized. Taking the battery-life of EVs into account, the maximum switching between charge and discharge states has been limited via constraint (5). Using Eq. (6) the SOC of EVs is calculated. Also, the SOC of EVs should be restricted in its minimum and maximum limits which is modeled by constraint (7) [26]. In addition, constraint (8) is implemented to model the maximum charge/discharge rates of EVs considering different charging time of utilized batteries in EVs which is an important parameter in scheduling of the IPL. To make sure that the SOC of EVs is in requested level at departure, constraint (9) is utilized. Finally, the SOC of EVs at each time should be equal or greater to the EVs' SOC when entering which is modeled via constraint (10) [18].

2.3. Modeling of renewable energy sources

Generated power by the WT which is dependent on the wind speed is modeled by constraint (11) [27]. Power output of PV system which is related to temperature and solar radiation is calculated by constraint (12).

$$P^{k,t}_{W} = \begin{cases} 0 & V^{t} < V^{k}_{c} \text{ or } V^{t} \ge V^{k}_{F} \\ \frac{V^{t} - V^{k}_{c}}{V^{k}_{R} - V^{k}_{c}} \times P^{k}_{R} & V^{k}_{c} \le V^{t} < V^{k}_{R} \\ P^{k}_{R} & V^{k}_{R} \le V^{t} < V^{k}_{F} \end{cases} \tag{11}$$

$$P^{p,t}_{PV} = \eta^{p} \times s^{p} \times G^{t} \times (1 - 0.005 \times (T_{a} - 25)) \tag{12}$$

where,

Indices

k, p Indicators of wind generation and PV system
Parameters
P^{k}_{R}, $P^{k,t}_{W}$ WT's rated and output power
V^{k}_{c}, V^{k}_{R}, V^{k}_{F} WT's cut-in, rated and cut-out speed s
V^{t} Forecasted wind speed
$P^{p,t}_{PV}$ PV's output power
η^{p} PV's conversion efficiency
s^{p}, T_{a} Area of PV and temperature
G^{t} Solar irradiation

2.4. Modeling of MTs

Technical constraints of MTs are provided by Eqs. (13)-(23).

$$C_{LDG}^{j,t} = a^j \times U^{j,t} + b^j \times P_{LDG}^{j,t} \tag{13}$$

$$SC_{LDG}^{j,t} \geq (U^{j,t} - U^{j,t-1}) \times UDC^j$$
$$SC_{LDG}^{j,t} \geq 0 \tag{14}$$

$$SHC_{LDG}^{j,t} \geq (U^{j,t-1} - U^{j,t}) \times SDC^j$$
$$SHC_{LDG}^{j,t} \geq 0 \tag{15}$$

$$P_{LDG}^{j,t} \leq P_{LDG,\max}^{j} \times U^{j,t} \tag{16}$$

$$P_{LDG}^{j,t} \geq P_{LDG,\min}^{j} \times U^{j,t} \tag{17}$$

$$P_{LDG}^{j,t} - P_{LDG}^{j,t-1} \leq RU^j \times U^{j,t} \tag{18}$$

$$P_{LDG}^{j,t-1} - P_{LDG}^{j,t} \leq RD^j \times U^{j,t-1} \tag{19}$$

$$U^{j,t-1} - U^{j,t} \leq 1 - U^{j,t+Dn_{j,f}} \tag{20}$$

$$U^{j,t} - U^{j,t-1} \leq U^{j,t+Up_{j,f}} \tag{21}$$

$$\mathrm{Dn_{j,f}} = \begin{Bmatrix} f & f \leq \mathrm{MDT_j} \\ 0 & f > \mathrm{MDT_j} \end{Bmatrix} \tag{22}$$

$$\mathrm{Up_{j,f}} = \begin{Bmatrix} f & f \leq \mathrm{MUT_j} \\ 0 & f > \mathrm{MUT_j} \end{Bmatrix} \tag{23}$$

where,
Indices

fAuxiliary index for modeling of DG's minimum OFF-time and ON-time starting from 1 to the high value of {$\mathrm{mut_j}$, $\mathrm{mdt_j}$}.
Parameters
a^j, b^jCoefficients for DG's operation cost function
UDC^jDG's start-up cost
SDC^jDG's shut-down cost
$P_{LDG,\max}^{j}$, $P_{LDG,\min}^{j}$ DG's maximum and minimum power
RD^j,RU^jRamp down /up amount of DG
MUT_j, MDT_jDG's minimum up/down times
Decision variables
$U^{j,\ t}$Binary variable, which is equal to 1 if MT is ON; otherwise 0
$P_{LDG}^{j,t}$DG's scheduled power
$Dn_{\mathrm{j,\ f}}$, $\mathrm{Up_{j,\ f}}$Auxiliary positive variable for modeling DG's minimum down/up time limit

Eqs. (13)-(15) models the operation, start-up and shut-down costs of MTs, respectively [19]. Operating constraints of MTs are presented by Eqs. (16)-(23). Eqs. (16) and (17) models maximum and minimum generated power limits, Eqs. (18) and (19) models ramp up and down constraints, and Eqs. (20) and (21) presents minimum down-time and up-time constraints of the MTs, respectively. Lastly, Eqs. (22) and (23) is used to linearize minimum down-time and up-time limitations of MTs [19].

2.5. Constraint of upstream network

The exchanged energy between the upstream network and IPL is limited in Eq. (24) [19].

$$|P_{UG}^{t}| \leq P_{UG}^{\max} \tag{24}$$

where,
Parameter

$P_{UG}^{\max}$ Maximum limit of power exchange between the upstream network and IPL

2.6. DRP modeling

Eqs. (25)-(28) are utilized to implement time-of-use rate of DRP. In this program, it is assumed that some load can be transferred from peak-periods to off-peak periods which smooth outs the load-curve while aggregation of consumed energy is not reduced during time-horizon of the study [24].

$$load^t = load_0^t + DRP^t \tag{25}$$

$$DRP^t \leq +DRP^{\max} \times load_0^t \tag{26}$$

$$DRP^t \geq -DRP^{\max} \times load_0^t \tag{27}$$

$$\sum_{t=1}^{T} DRP^t = 0 \tag{28}$$

where,
Parameter

$load_0^t$, $DRP^{\max}$ Load amount and maximum load participation in DRP
Decision variables
$load^t$Load profile after implementing DRP
DRP^tFree variable for DRP implementation which is positive when load is increased and negative when load is decreased

After DRP implementing, the amount of load is determined using Eq. (25). Using Eqs. (26) and (27), the amount of transferred power from one period to another is restricted. In this study, it is assumed that only 20% of base load at each hour can be transferred to other periods. To ensure that the load demand is just transferred from peak periods to off-peak periods, Eq. (28) is utilized [28].

2.7. Hydrogen storage system modeling

A hydrogen storage system (HSS) which is composed of hydrogen storage tanks, FC, and EL is considered in the case study [29]. In the considered HSS, the electrolyser converts energy to hydrogen molar during low-price time periods which is stored and filled the hydrogen tank. Then, hydrogen stored in the tank is turned to energy during high price periods. Eqs. (29)-(41) model the operation of the HSS [30].

$$P_t^{EL} \leq P_{\max}^{EL} \times U_t^{EL} \tag{29}$$

$$P_t^{EL} \geq P_{\min}^{EL} \times U_t^{EL} \tag{30}$$

$$N_{H2,t}^{EL} \leq N_{H2,\max}^{EL} \times U_t^{EL} \tag{31}$$

$$N_{H2,t}^{EL} = \frac{\eta^{EL} P_t^{EL}}{LHV_{H2}} \tag{32}$$

$$P_{t0}^{H2} = P_{initial}^{H2} \tag{33}$$

$$P_t^{H2} \leq P_{\max}^{H2} \tag{34}$$

$$P_t^{H2} \geq P_{\min}^{H2} \tag{35}$$

$$N_{H2,t}^{FC} \leq N_{H2,\max}^{FC} \times U_t^{FC} \tag{36}$$

$$N_{H2,t}^{FC} = \frac{P_t^{FC}}{\eta^{FC} LHV_{H2}} \tag{37}$$

$$P_t^{FC} \leq P_{\max}^{FC} \times U_t^{FC} \tag{38}$$

$$P_t^{FC} \geq P_{\min}^{FC} \times U_t^{FC} \tag{39}$$

$$U_t^{EL} + U_t^{FC} \leq 1 \tag{40}$$

$$P_t^{H2} = P_{t-1}^{H2} + \frac{\Re T_{H2}}{V_{H2}}(N_{H2,t}^{EL} - N_{H2,t}^{FC}) \tag{41}$$

where,

Parameters

$\Re$, T_{H2}, LHV_{H2}Constant of gas, average temperature and minimum heating amount of hydrogen
$N_{H2,\max}^{EL}$, $N_{H2,\max}^{FC}$ Maximum limit of hydrogen molar production and consumption in the electrolyser (EL) and fuel cell (FC), respectively
$P_{\min}^{EL}$, $P_{\max}^{EL}$ Minimum and maximum limits of power consumption in the EL
$P_{\min}^{FC}$, $P_{\max}^{FC}$ Minimum and maximum limits of power production in the FC
$P_{initial}^{H2}$, P_{t0}^{H2}Hydrogen tank's pressure in the starting time
$P_{\max}^{H2}$, $P_{\min}^{H2}$ Hydrogen tank's maximum and minimum pressure limits
V_{H2}Overall tank volume
η^{FC}, η^{EL}FC/EL's efficiency
Decision variables
$N_{H2,t}^{FC}$, $N_{H2,t}^{EL}$FC/EL's hydrogen molar consumption/production
P_t^{H2}Pressure of hydrogen tank
P_t^{EL}, P_t^{FC}EL/FC's power consumption/production
U_t^{FC}, U_t^{EL}Binary variable for FC/EL's ON or OFF modes

The maximum and minimum power consumption constraints of the electrolyser are presented by constraints (29) and (30). Eq. (31) limits the maximum hydrogen molar generation of the electrolyser. Using Eq. (32), the generated hydrogen molar by the electrolyser can be calculated [30]. In addition, constraints (33)-(35) model the initial amount of pressure, maximum and minimum amounts of hydrogen tank, respectively [30]. Furthermore, the maximum hydrogen molar consumption of the fuel cell is limited by Eq. (36). Consumed hydrogen by the fuel cell, $N_{H2,t}^{FC}$, to generate power, P_t^{FC}, is calculated by Eq. (37). Finally, in order to restrict amount of generated power by the fuel cell, Eqs. (38) and (39) is utilized. In order to prevent simultaneous operation of the electrolyser and fuel cell, Eq. (40) is provided. Finally, Eq. (41) presents the dynamic model of HSS [30].

2.8. Power balance constraint

Constraint (42) is used to make a balance between consumed and procured power by the IPL. The new load demand after implementing DRP is used rather than initial load amount in the power balance constraint.

$$P_{UG}^t + \sum_{k=1}^{K} P_W^{k,t} + \sum_{p=1}^{P} P_{PV}^{p,t} + \sum_{j=1}^{G} P_{LDG}^{j,t} + \sum_{i=1}^{N} P_{Dch,EV}^{i,t} + P_t^{FC} = load^t + \sum_{i=1}^{N} P_{Ch,EV}^{i,t} + P_t^{EL} \tag{42}$$

3. The background of IGDT technique

Various valuable approaches such as stochastic, fuzzy modeling, robust-optimization, and IGDT method are developed to model uncertainty in any system. IGDT is firstly proposed by Prof. Ben-Haim in [31]. To compare the IGDT technique with similar approach like robust optimization, IGDT technique analysis the worst and the best strategies to deal with but robust optimization only deals with worst strategy. It should be noted that any uncertain parameter might have negative or positive impacts on the system. Therefore, the IGDT method is utilized as a proper method to evaluate both negative and positive sides of an uncertainty by considering robustness and opportunity functions, respectively, which is impossible using other methods. Using the IGDT method, three strategies as risk-taker, risk-neutral, and risk-averse are developed in which the system operators can get better interception of impacts of uncertainty of power price in the upstream grid and get optimum decision based on their preferences. In the previous studies, IGDT is applied to obtain optimal bidding strategy of large consumer in [32] and central concentrating solar power plant in [33].

The problem formulation in the presence of upstream grid price uncertainty model is briefly expressed in Eqs. (43)-(47) which λis the uncertainty parameter.

$$f_b = \min(f(X, \pi_{UG}^t)) \tag{43}$$

$$H(X) \le 0 \tag{44}$$

$$G(X) = 0 \tag{45}$$

$$\pi_{UG}^t \in U \tag{46}$$

$$U(\alpha, \tilde{\pi}_{UG}^t) = \left\{ \pi_{UG}^t : \frac{|\pi_{UG}^t - \tilde{\pi}_{UG}^t|}{\tilde{\pi}_{UG}^t} \le \alpha \right\} \alpha \ge 0 \tag{47}$$

In above equations, $X$and U show the decision variables and set of uncertainty in the model, respectively. Eq. (47) expresses the uncertainty model mathematically, which is based on fractional error model from IGDT technique [31]. The parameters α and $\tilde{\pi}_{UG}^t$ are the uncertain radius and the forecasted amount of uncertain parameter. In other words, α is the maximum deviation value of uncertain parameter from its forecasted value. The three risk-based strategies in IGDT technique are expressed as follows:

3.1. Risk-neutral strategy

When the uncertainty parameter is forecasted exactly to its certain values, the uncertainty has no effect on objective function. The mathematical model for risk-neutral strategy is formulated below.

$$f_b = \min(f(X, \tilde{\pi}_{UG}^t)) \tag{48}$$

$$H(X) \le 0 \tag{49}$$

$$G(X) = 0 \tag{50}$$

The formulation of risk-neural strategy is based on zero deviation of uncertain parameter from its exact amount.

3.2. Risk-averse strategy based on robustness function of IGDT

Power price rising in the upstream network is modeled by the robustness function. To get robust operation of the system, $\hat{\alpha}(r_c)$ determines the maximum resistance against any rising of power price in the upstream network. In this case, the system operator by spending more money on energy procurement seeks to get the risk-averse strategy. To get $\hat{\alpha}(r_c)$value, optimization problem (51)-(57) should be optimized.

$$\hat{\alpha}(r_c) = \max \alpha \tag{51}$$

$$f(X, \pi_{UG}^t) \le r_c \tag{52}$$

$$r_c = f_b(X, \tilde{\pi}_{UG}^t) \times (1 + \mu) \tag{53}$$

$$H(X) \le 0 \tag{54}$$

$$G(X) = 0 \tag{55}$$

$$\frac{|\pi_{UG}^t - \tilde{\pi}_{UG}^t|}{\tilde{\pi}_{UG}^t} \le \alpha \tag{56}$$

$$0 \le \mu \le 1 \tag{57}$$

Robustness function based on IGDT technique is provided in Eq. (51) which should be optimized subject to constraints (52)-(57). As provided above, the $\hat{\alpha}(r_c)$ is the maximum radius of uncertainty parameter and r_c is the predetermined amount of objective function and will be determined by the operator or decision maker. In addition, μ is the percentage of increased cost due to uncertainty parameter modeling.

3.3. Risk-taker strategy based on opportunity function of IGDT

To model power price decrease in the upstream network, the opportunity function of IGDT technique is utilized as risk-taker strategy. In other words, the deviation of uncertain parameter has positive effects on objective function. In this case, lower values of $\hat{\beta}(r_w)$ is desirable. Optimization problem (58)-(64) express the opportunity function based on IGDT.

$$\hat{\beta}(r_w) = \min \alpha \tag{58}$$

$$f(X, \pi_{UG}^t) \leq r_w \tag{59}$$

$$r_w = f_b(X, \tilde{\pi}_{UG}^t) \times (1 - \sigma) \tag{60}$$

$$H(X) \leq 0 \tag{61}$$

$$G(X) = 0 \tag{62}$$

$$\frac{|\pi_{UG}^t - \tilde{\pi}_{UG}^t|}{\tilde{\pi}_{UG}^t} \leq \alpha \tag{63}$$

$$0 \leq \sigma < 1 \tag{64}$$

Opportunity function based on IGDT technique is provided in Eq. (58) which should be optimized subject to constraints (59)-(64). The $r_w$is the minimum reduction value of objective function from its based determined amount and $\hat{\beta}$ has positive value and defined as minimum radius of uncertainty. The σ is also determined by operator or decision maker.

4. An IGDT risk-involved problem formulation

4.1. Risk-averse strategy via robustness function of IGDT

To get risk-averse strategy of the system via robustness function of IGDT, $\hat{\alpha}(r_c)$ determines the maximum resistance against any rising of power price in the upstream network. In this case, the system operator by spending more money on energy procurement seeks to get the risk-averse strategy.

The risk-averse strategy of the system via robustness function of IGDT is formulated as follows:

$$\hat{\alpha}(r_c) = \max \alpha \tag{65}$$

Subject to:

$$\left\{ \sum_{t=1}^{T} \left[\begin{pmatrix} P_{UG}^t \times \pi_{UG}^t + \sum_{j=1}^{G} (C_{LDG}^{j,t} + SC_{LDG}^{j,t} + SHC_{LDG}^{j,t}) \\ + \sum_{i=1}^{N} (-P_{Ch,EV}^{i,t} \times \pi_{Ch,EV}^{i} + P_{Dch,EV}^{i,t} \times \pi_{Dch,EV}^{i}) \end{pmatrix} \times \Delta t \right] \right\} \leq r_c \tag{66}$$

$$\pi_{UG}^t = (1 + \alpha) \times \tilde{\pi}_{UG}^t \tag{67}$$

$$\text{Constraints}\,(2) - (42) \tag{68}$$

$$\tilde{P}_{UG}^t > P_{UG}^t;\ \tilde{\pi}_{UG}^t < \pi_{UG}^t \tag{69}$$

It should be noted that the constraint (69) is added to construct optimal bidding curves which is submitted to the upstream grid to purchase power.

4.2. Risk-neutral strategy without considering IGDT technique

The amount of forecasted upstream grid price is the same as the real value and the formulations are as follows:

$$\textit{Minimizing} \left\{ \sum_{t=1}^{T} \left[\begin{pmatrix} P_{UG}^t \times \pi_{UG}^t + \sum_{j=1}^{G} (C_{LDG}^{j,t} + SC_{LDG}^{j,t} + SHC_{LDG}^{j,t}) \\ + \sum_{i=1}^{N} (-P_{Ch,EV}^{i,t} \times \pi_{Ch,EV}^{i} + P_{Dch,EV}^{i,t} \times \pi_{Dch,EV}^{i}) \end{pmatrix} \times \Delta t \right] \right\} \tag{70}$$

$$\pi_{UG}^t = \tilde{\pi}_{UG}^t \tag{71}$$

Subject to:

$$\text{Constraints}\,(2) - (42) \tag{72}$$

4.3. Risk-taker strategy via opportunity function of IGDT

To model power price decrease in the upstream network, the opportunity function of IGDT technique is utilized. In this case, lower values of $\hat{\beta}(r_w)$is desirable.

The risk-taker strategy of the system via opportunity function of IGDT is formulated as follows:

$$\hat{\beta}(r_w) = \min \alpha \tag{73}$$

Subject to:

$$\left\{ \sum_{t=1}^{T} \left[\begin{pmatrix} P_{UG}^t \times \pi_{UG}^t + \sum_{j=1}^{G} (C_{LDG}^{j,t} + SC_{LDG}^{j,t} + SHC_{LDG}^{j,t}) \\ + \sum_{i=1}^{N} (-P_{Ch,EV}^{i,t} \times \pi_{Ch,EV}^{i} + P_{Dch,EV}^{i,t} \times \pi_{Dch,EV}^{i}) \end{pmatrix} \times \Delta t \right] \right\} \leq r_w \tag{74}$$

$$\pi_{UG}^t = (1 - \alpha) \times \tilde{\pi}_{UG}^t \tag{75}$$

$$\text{Constraints}\,(2) - (42) \tag{76}$$

$$\tilde{P}_{UG}^t < P_{UG}^t;\ \tilde{\pi}_{UG}^t > \pi_{UG}^t \tag{77}$$

It should be noted that the constraint (77) is added to construct optimal bidding curves which is submitted to the upstream grid to purchase power.

5. Numerical simulation

In this paper, the main scope is to construct optimal bidding curve to be submitted in the upstream grid by the operator of the IPL taking impacts of HSS and DRP into account. On the other hand, optimal scheduling of the different components of the system is studied considering uncertainty of power price. Therefore, the results have been presented in risk-taker, risk-neutral, and risk-averse which are corresponded to opportunity, deterministic, and robustness functions of IGDT technique. In addition, at each strategy, to show the effectiveness of the DRP, with and without DRP cases is considered to solve the problem. All the required information for the simulation has been taken from Jannati and Nazarpour [34]. Simulations are implemented under GAMS optimization software [35] and solved using DICOPT solver [36].

5.1. Risk-averse strategy of the system

By using the robustness-function based on IGDT technique, any increase in the power price is modeled and its impact on the scheduling of different elements of the system can be comprehensively investigated. Therefore, robustness function results are used to develop the risk-averse strategy. In this strategy, the system operator seeks to be immune to the high power prices in the upstream-grid by using its internal sources. Fig. 2 depicts the robust operating cost of the system against the robustness parameter $\hat{\alpha}(r_c)$. It is seen that by increasing total operating cost of the system, the robustness parameter in both without and with DRP cases is continuously increasing. This means that higher

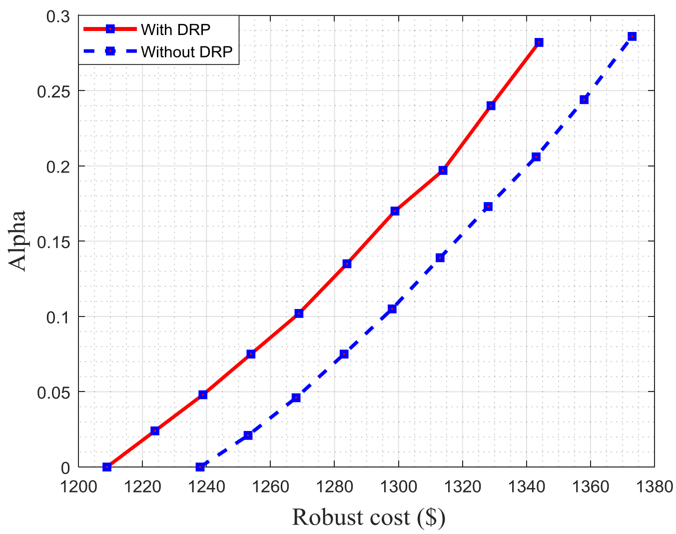

Fig. 2. Robustness-function based on IGDT technique.

robustness in operation of system considering increase in the power price, more money should paid as the operating cost of the system. In addition, it can be seen that by implementing DRP, obtained robustness is considerably increased. For example, by considering $1320 as operating cost of the system the robustness of the system is about 15% in without DR case, while this number is increased to 20% by implementing DR case.

5.2. Risk-taker strategy of the system

As said before, the opportunity function based IGDT technique is used to get analysis of possible power price reduction in the power systems. In this study, any reduction in power price will lead to a windfall profit in operation of the system. To get precise interception of obtained results on the operation of the system, risk-taker strategy is obtained based on opportunity function results. The opportunity function versus the operating cost of the system is illustrated in Fig. 3. It is shown that total opportunistic operating cost against the opportunity parameter is continuously descending. This means that higher risks against the uncertainty by considering the lower operating cost. According to Fig. 3, by considering 15% for opportunity function, the total operating cost of the system approximately will be equal to $1120 and $1100 for without and with DRP cases.

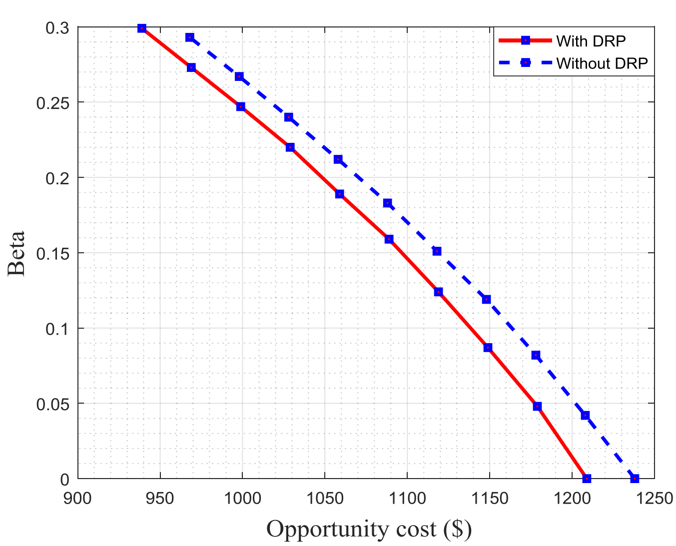

Fig. 3. Opportunity-function based on IGDT technique.

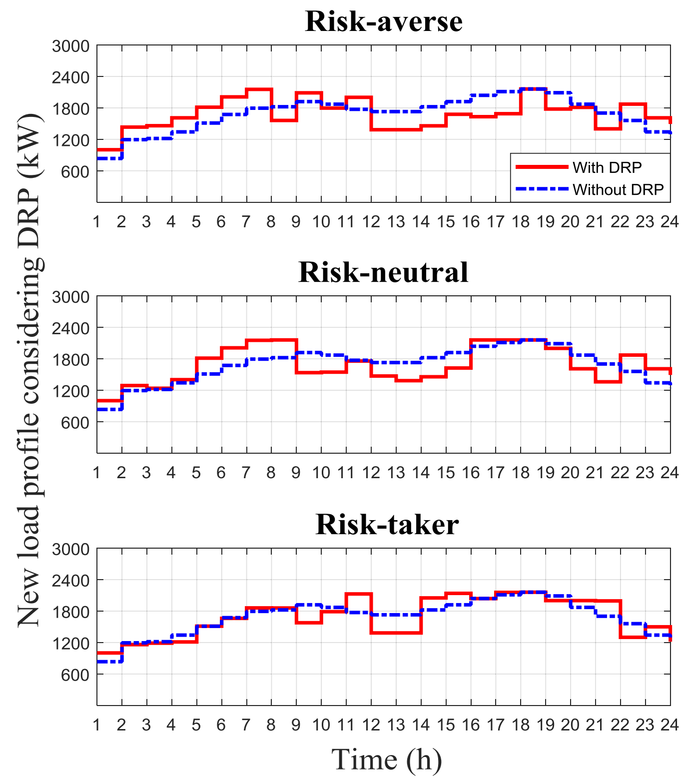

Fig. 4. Load demand after implementing DRP.

5.3. Load profile

By applying DRP, the load demand is transferred from high price time periods to low price time periods to flatten the load curve which will result in lower operating costs. Fig. 4 presents the load curve of the system in three strategies. In is obvious that the load demand is increased during early hours of the day because reasonable power price is offered in the upstream grid. In contrast, during hours 17–23 where higher power prices are experienced in the upstream grid, the load demand is reduced in all strategies by applying demand response program at this period. In risk-averse strategy to avoid high risks of power price, amount of shifted demand is higher than two other strategies. In opposite way, the minimum amount of load transition between low and high price period is recorded in the risk-taker strategy due to take advantage of possible power price decrease in the upstream network.

5.4. Power generation of MTs

As discussed before, to satisfy required load demand of the system, three different MT units are considered as internal power sources in the system. Power generation of these units is depicted in Figs. 5-7. According to Fig. 5 which shows the power generation of MT1, in risk-averse strategy, this unit generate power under its maximum capacity to help the system operator to be reduce power procurement from the upstream network. Turning to Fig. 4 shows that by implementing DR program load is shifted to hours 1–6 in this strategy; therefore, generated power by MT1 is increased to satisfy load after applying DR program in risk-averse strategy while power generation of other units is not changed or even decreased.

In risk-neutral strategy, power generation of MT2, which is shown in Fig. 6, is increased after implementing DR programs. In contrast, as it can be shown from Fig. 7, generated power by the MT3 is equal to zero when DR program is applied while there is not significant change in generated power by the MT1 in this case.

To get advantage of lower electricity prices in the upstream

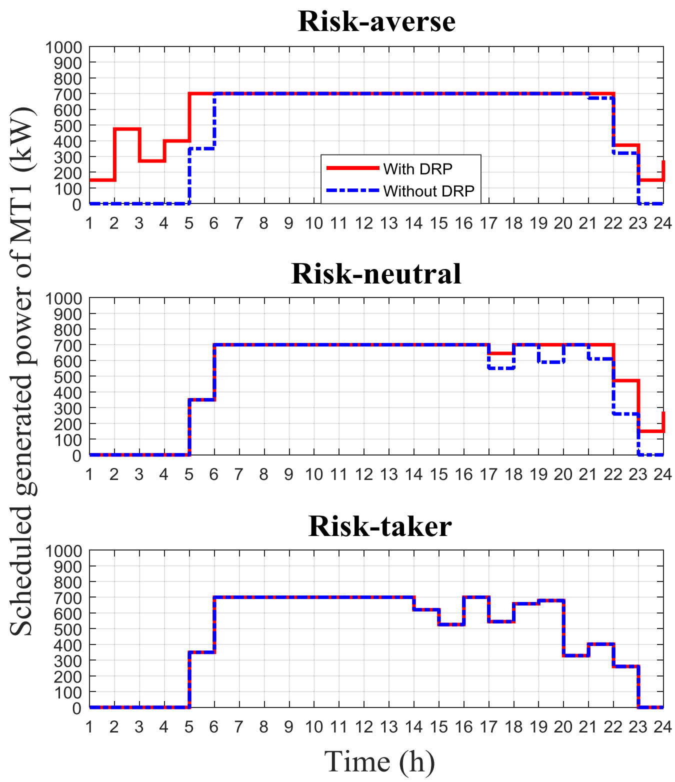

Fig. 5. Scheduled generated power of MT1.

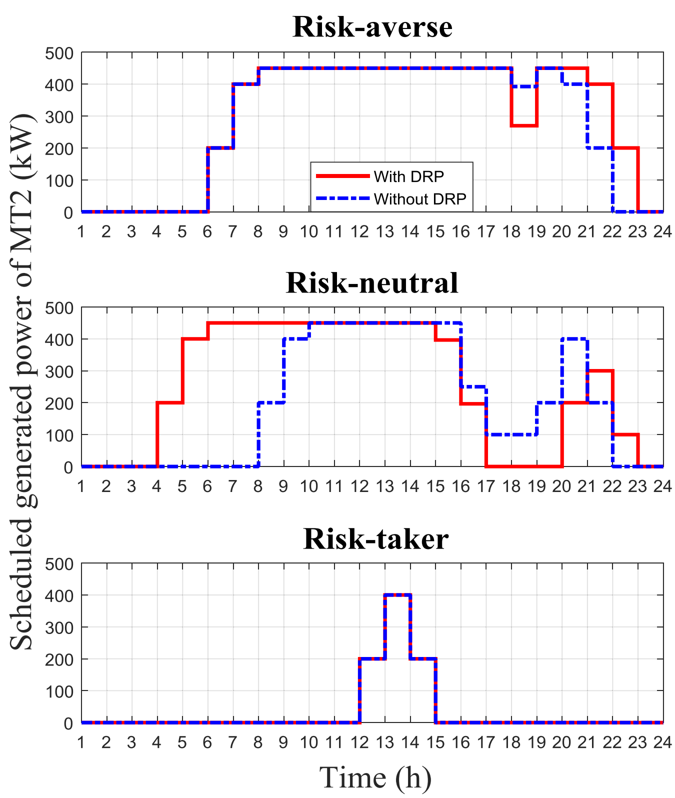

Fig. 6. Scheduled generated power of MT2.

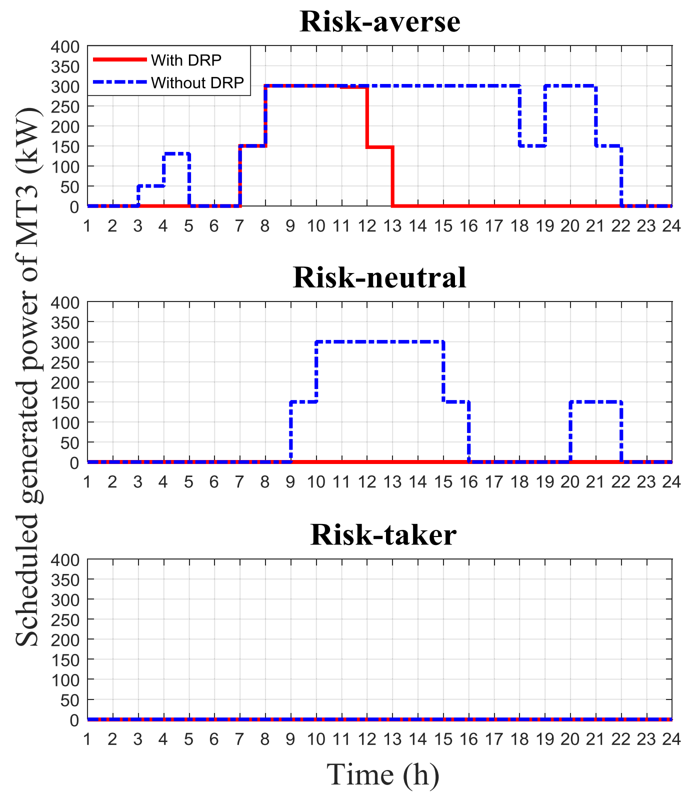

Fig. 7. Scheduled generated power of MT3.

network, the system operator prefers to purchase power from upstream network than using its internal resources. Therefore, scheduled power generation of MTs in risk-taker strategy is much less than generated power in other two strategies in which the MT3 is not scheduled to generate power in this strategy. In addition, it is seen that implementing DR program has no made significant difference in scheduling of the MTs in the risk-taker strategies. Finally, as was expected, comparing obtained results show that the maximum generated power by the MTs is recorded in risk-averse strategy while the minimum amount of scheduled power of these units is reported in risk-averse strategy.

5.5. Operation of the IPL

Average SOC of the IPL is shown in Fig. 8. According to Fig. 8, it can be interfered that parked EVs in the IPL have not been charged or discharged between hours 1–5 in risk-neutral strategy and risk-taker strategy as their SOC's has not changed. In all strategies, the EVs have been charged during hours 6–17 in which their SOC level has been increased from 40% to about 90%. Fig. 9 depicts discharging and charging power of the IPL which approves the previous explanations.

5.6. Operation of HSS

The charged and discharged power of HSS is illustrated in Fig. 10. It should be noted that charged power is shown by positive numbers while the discharged power is provided by negative numbers. In all strategies the HSS is charged at early and late hours of the time horizon because the load demand and power price are low. On the other hand, hours 19 and 20 when the load demand is high, the HSS injects power to the system in risk-taker and risk-averse strategies, respectively. In risk-taker strategy, in with DR case, the HSS only is discharged during hours 12–14.

5.7. Optimal bidding curves

To take part in the power market and power procurement from the upstream network, submitting offering and bidding curves to the power market is necessary. According to a common requirement in almost any power markets, the offering and bidding curves should be steadily

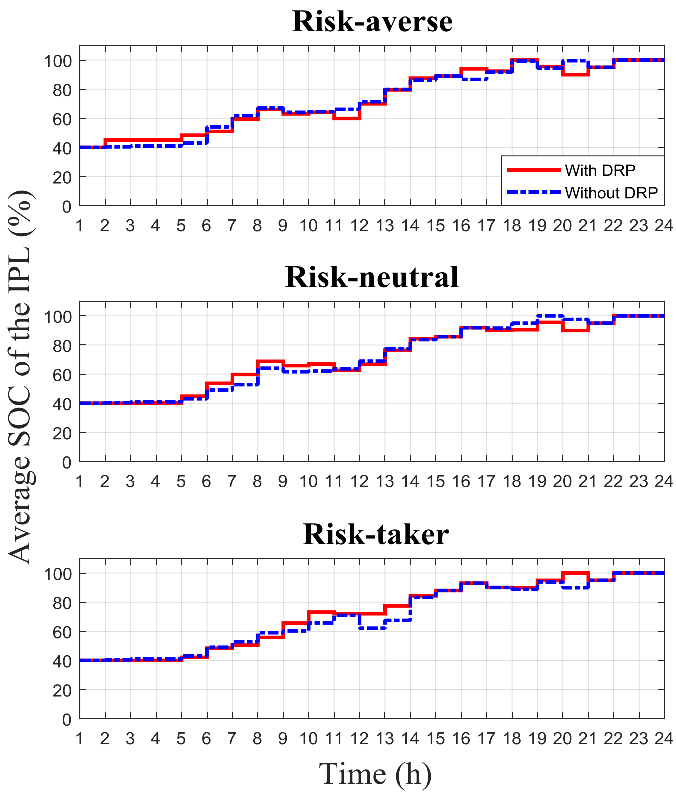

Fig. 8. Average SOC of the IPL (%).

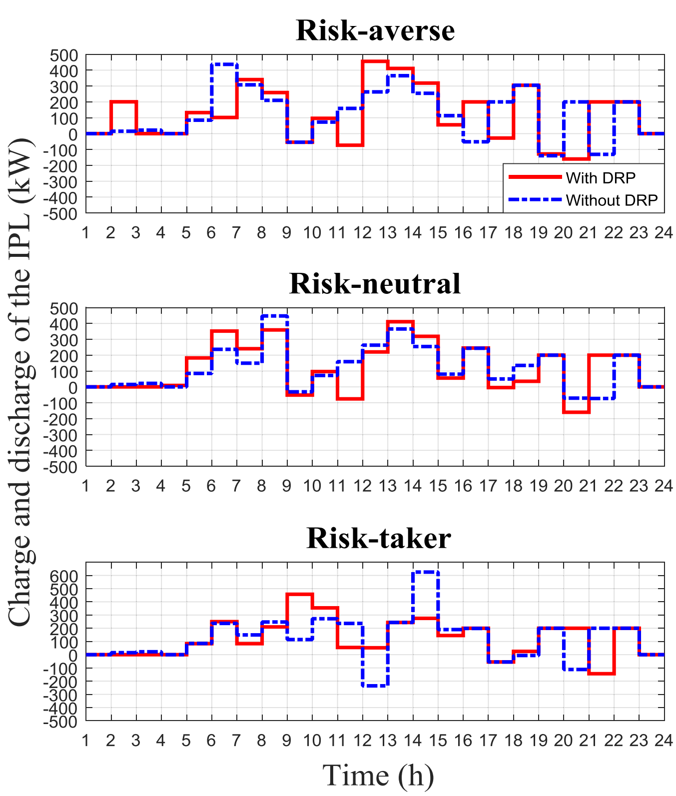

Fig. 9. Discharging and charging power of EVs in the IPL.

increasing and decreasing, respectively. When there is an uncertainty in the power market, providing bidding curves helps the system operator to purchase power from upstream network at the best possible prices. Therefore, at each hour, the bidding curves should be provided and

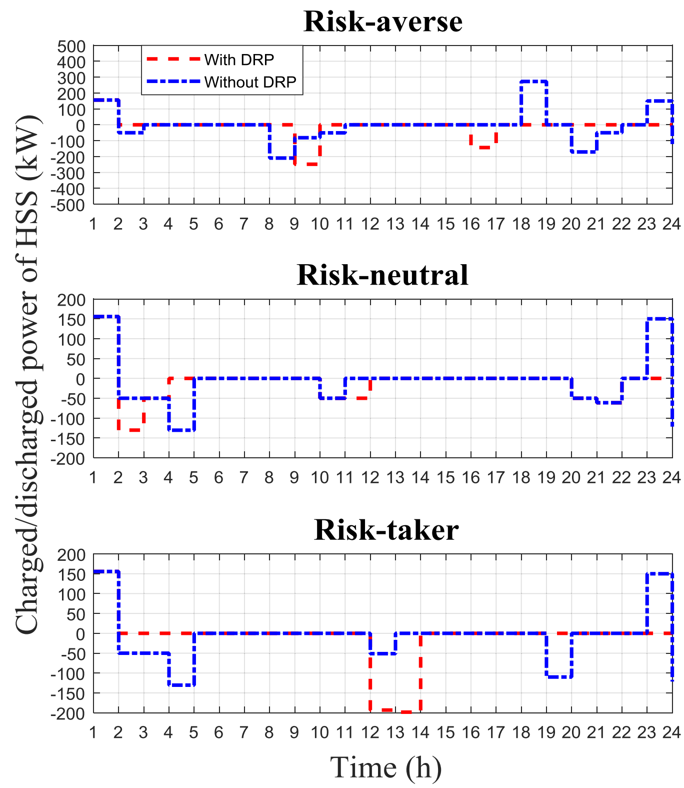

Fig. 10. Charged and discharged power of the HSS.

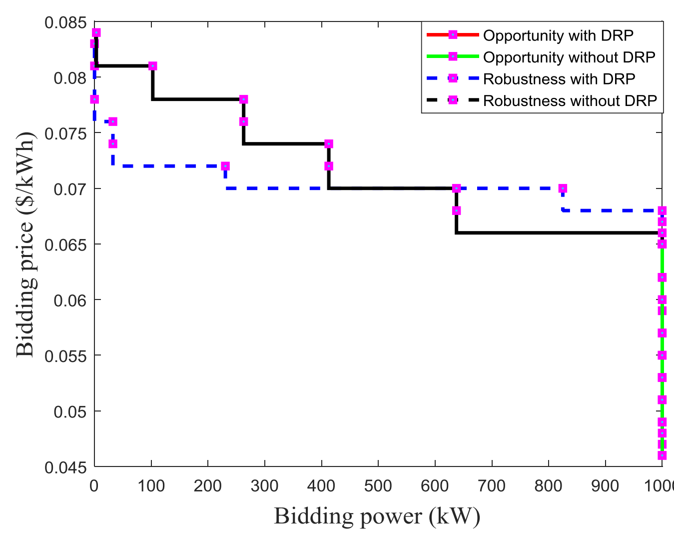

Fig. 11. Optimal bidding curve at hour 8.

submitted to the market. In this paper, the optimal bidding curve at each hour is developed in four different cases as opportunity with DRP, opportunity without DRP, robustness with DRP, and robustness without DRP to cover all the possible situations. Fig. 11 illustrates the optimal bidding curve of the system at hour 8. As it can be shown, in all cases, when the bidding price is higher than 0.08 $/kWh the bidding power is equal to zero. In other words, in opportunity with and without DRP cases, when the bidding price drops to less than 0.065 $/kWh, the bidding power reaches its maximum level which is 1000 kW.

Fig. 12 presents the optimal bidding curves at hour 14. At this hour bidding power in robustness with and without DRP cases is equal to zero which means that the power prices in the market is not reasonable according to the robustness strategy of the system operator. In opportunity with DRP case, bidding power is zero which price is higher than

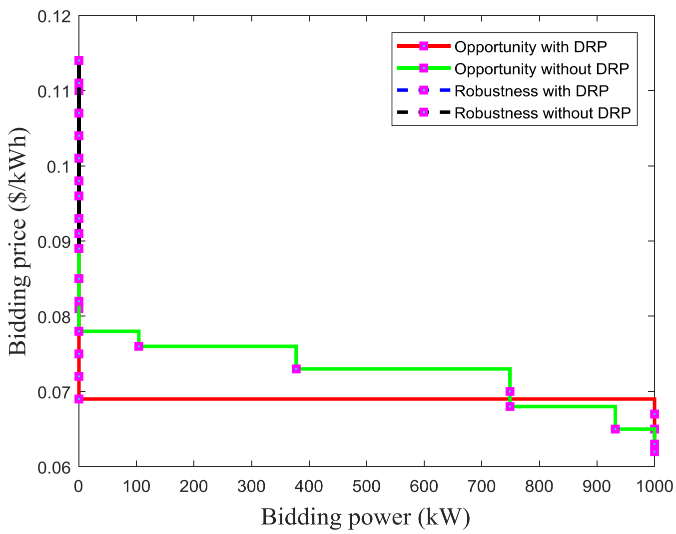

Fig. 12. Optimal bidding profile at hour 14.

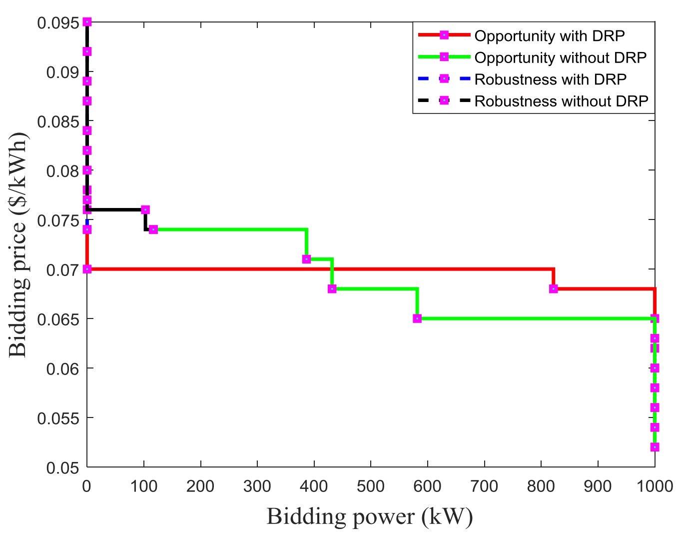

Fig. 13. Optimal bidding curve at hour 15.

0.069 $/kWh while by reaching bidding price to under this level, the bidding power is increase to its maximum level. In addition, in opportunity without DRP case, by reducing bidding prices to 0.076 $/kWh, the system operator increased its bidding power to procure power from the upstream network.

Optimal bidding curve of the system of hour 15 is depicted in Fig. 13. At this hour, bidding power in robustness with DR case is equal to zero for all power prices while 102.7 kW at price 0.076 $ and 116.7 kW at price $0.074 at this hour is bided by the system operator in robustness without DR case. Finally, in opportunity with and without cases, the bidding power is equal to 1000 kW when bidding price is less than $0.063 at this hour.

6. Conclusion

In this work, developing a new method to get optimal bidding curves and optimal energy management of IPL in the presence of the HSS considering DRP has been investigated in an uncertain power market structure. DRP is taken into account as a virtual generation unit. To model power price uncertainty and develop optimal bidding curve, the opportunity and robustness functions based on IGDT technique has been developed. Obtained results has been presented in three strategies namely risk-taker, risk-neutral, and risk-averse corresponding to opportunity, deterministic, and robustness functions of the IGDT technique, each of which, has been solved in two cases as with and without DRP cases. Furthermore, the optimal bidding curve and optimal scheduling of different elements of the system is discussed in the context. Finally, in the future work, robust optimization method can be applied to obtain optimal energy management and optimal bidding curves of IPL in the presence of the HSS and DRP in an uncertain environment.

CRediT authorship contribution statement

Jun Liu: Conceptualization, Data curation, Writing - original draft, Writing - review & editing. **Chong Chen:** Conceptualization, Data curation, Writing - original draft, Writing - review & editing. **Zhenling Liu:** Conceptualization, Data curation, Writing - original draft, Writing - review & editing. **Kittisak Jermsittiparsert:** Conceptualization, Data curation, Writing - original draft, Writing - review & editing. **Noradin Ghadimi:** Conceptualization, Data curation, Writing - original draft, Writing - review & editing.

Declaration of Competing Interest

This manuscript has not been submitted to, nor is under review at, another journal or other publishing venue.

The authors have no affiliation with any organization with a direct or indirect financial interest in the subject matter discussed in the manuscript

Acknowledgements

This research had been supported by Program for Science & Technology Innovation Talents in Universities of Henan Province under Grant No.19HASTIT031, National Social Science Foundation under Grants No.19BGL034, Humanities and Social Sciences Planning Project of Ministry of Education under Grant No.18YJC630006, Soft Science Research Planning Project of Henan Province under Grant No.192400410248, Key Scientific Research Project of Universities and Colleges in Henan Province under Grant No.19B630001, Major Project of Philosophy and Social Sciences Application Research in Higher Education Institutions from Henan Province under Grant No.2017-YYZD-03, Support Plan for Science & Technology Innovation Talents in Universities of Henan Province (Humanities and Social Sciences) under Grant No.2019-CX-022, Young talents Fund of HUEL.

Supplementary materials

Supplementary material associated with this article can be found, in the online version, at doi:10.1016/j.est.2019.101057.

References

[1] M. Mohiti, H. Monsef, H. Lesani, A decentralized robust model for coordinated operation of smart distribution network and electric vehicle aggregators, Int. J. Electr. Power Energy Syst. 104 (uary) (2019) 853–867.
[2] A. Alahyari, M. Ehsan, M. Mousavizadeh, A hybrid storage-wind virtual power plant (VPP) participation in the electricity markets: a self-scheduling optimization considering price, renewable generation, and electric vehicles uncertainties, J. Energy Storage 25 (ober) (2019) 100812.
[3] M. Sedighizadeh, G. Shaghaghi-shahr, M. Esmaili, M.R. Aghamohammadi, Optimal distribution feeder reconfiguration and generation scheduling for microgrid day-ahead operation in the presence of electric vehicles considering uncertainties, J. Energy Storage 21 (ruary) (2019) 58–71.
[4] M. Esmaili, H. Shafiee, J. Aghaei, Range anxiety of electric vehicles in energy management of microgrids with controllable loads, J. Energy Storage 20 (ember) (2018) 57–66.
[5] R. Razipour, S.M. Moghaddas-Tafreshi, P. Farhadi, Optimal management of electric vehicles in an intelligent parking lot in the presence of hydrogen storage system, J. Energy Storage 22 (il) (2019) 144–152.
[6] S. Rezaee, E. Farjah, B. Khorramdel, Probabilistic analysis of plug-in electric vehicles impact on electrical grid through homes and parking lots, IEEE Trans. Sustain. Energy 4 (tember(4)) (2013) 1024–1033.

[7] L. Zhang, Y. Li, A game-theoretic approach to optimal scheduling of parking-lot electric vehicle charging, IEEE Trans. Veh. Technol. 65 (ober(6)) (2015) 4068–4078.
[8] L. Zhang, Y. Li, Optimal management for parking-lot electric vehicle charging by two-stage approximate dynamic programming, IEEE Trans. Smart Grid 8 (ember (4)) (2015) 1722–1730.
[9] M. Kuran, A.C. Viana, L. Iannone, D. Kofman, G. Mermoud, J.P. Vasseur, A smart parking lot management system for scheduling the recharging of electric vehicles, IEEE Trans. Smart Grid 6 (ch(6)) (2015) 2942–2953.
[10] M. Shafie-khah, E. Heydarian-Forushani, G.J. Osório, F.A. Gil, J. Aghaei, M. Barani, J.P. Catalão, Optimal behavior of electric vehicle parking lots as demand response aggregation agents, IEEE Trans. Smart Grid 7 (ember(6)) (2015) 2654–2665.
[11] M.J. Mirzaei, A. Kazemi, O. Homaee, A probabilistic approach to determine optimal capacity and location of electric vehicles parking lots in distribution networks, IEEE Trans. Ind. Inform. 12 (tember(5)) (2015) 1963–1972.
[12] E. Akhavan-Rezai, M.F. Shaaban, E.F. El-Saadany, F. Karray, Online intelligent demand management of plug-in electric vehicles in future smart parking lots, IEEE Syst. J. 10 (il(2)) (2015) 483–494.
[13] U.C. Chukwu, S.M. Mahajan, V2G parking lot with PV rooftop for capacity enhancement of a distribution system, IEEE Trans. Sustain. Energy 5 (tember(1)) (2013) 119–127.
[14] M. Yazdani-Damavandi, M.P. Moghaddam, M.R. Haghifam, M. Shafie-khah, J.P. Catalão, Modeling operational behavior of plug-in electric vehicles' parking lot in multienergy systems, IEEE Trans. Smart Grid 7 (ch(1)) (2015) 124–135.
[15] N. Neyestani, M.Y. Damavandi, M. Shafie-Khah, J. Contreras, J.P. Catalão, Allocation of plug-in vehicles' parking lots in distribution systems considering network-constrained objectives, IEEE Trans. Power Syst. 30 (ober(5)) (2014) 2643–2656.
[16] M. Jannati, S.H. Hosseinian, B. Vahidi, A significant reduction in the costs of battery energy storage systems by use of smart parking lots in the power fluctuation smoothing process of the wind farms, Renew. Energy 87 (ch) (2016) 1–4.
[17] H.A. Bonges III., A.C. Lusk, Addressing electric vehicle (EV) sales and range anxiety through parking layout, policy and regulation, Transport. Res. Part A 83 (uary) (2016) 63–73.
[18] M. Honarmand, A. Zakariazadeh, S. Jadid, Integrated scheduling of renewable generation and electric vehicles parking lot in a smart microgrid, Energy Convers. Manag. 86 (ober) (2014) 745–755.
[19] M. Honarmand, A. Zakariazadeh, S. Jadid, Self-scheduling of electric vehicles in an intelligent parking lot using stochastic optimization, J. Frankl. Inst. 352 (ruary(2)) (2015) 449–467.
[20] E.B. Iversen, J.M. Morales, H. Madsen, Optimal charging of an electric vehicle using a Markov decision process, Appl. Energy 123 (e) (2014) 1–2.
[21] A. Zakariazadeh, S. Jadid, P. Siano, Multi-objective scheduling of electric vehicles in smart distribution system, Energy Convers. Manag. 79 (ch) (2014) 43–53.
[22] F. Fazelpour, M. Vafaeipour, O. Rahbari, M.A. Rosen, Intelligent optimization to integrate a plug-in hybrid electric vehicle smart parking lot with renewable energy resources and enhance grid characteristics, Energy Convers. Manag. 77 (uary) (2014) 250–261.
[23] M. Moradijoz, M.P. Moghaddam, M.R. Haghifam, E. Alishahi, A multi-objective optimization problem for allocating parking lots in a distribution network, Int. J. Electr. Power Energy Syst. 46 (ch) (2013) 115–122.
[24] A. El-Zonkoly, L. dos Santos Coelho, Optimal allocation, sizing of PHEV parking lots in distribution system, Int. J. Electr. Power Energy Syst. 67 (2015) 472–477.
[25] J. Song, V. Krishnamurthy, A. Kwasinski, R. Molina, Analysis of the energy storage operation of electrical vehicles with a photovoltaic roof using a Markov chain model, 2012 IEEE Vehicle Power and Propulsion Conference, IEEE, 2012, pp. 820–825.
[26] M. Honarmand, A. Zakariazadeh, S. Jadid, Optimal scheduling of electric vehicles in an intelligent parking lot considering vehicle-to-grid concept and battery condition, Energy 65 (ruary) (2014) 572–579.
[27] B.S. Borowy, Z.M. Salameh, Optimum photovoltaic array size for a hybrid wind/PV system, IEEE Trans. Energy Convers. 9 (tember(3)) (1994) 482–488.
[28] A.N. Ghalelou, A.P. Fakhri, S. Nojavan, M. Majidi, H. Hatami, A stochastic self-scheduling program for compressed air energy storage (CAES) of renewable energy sources (RESs) based on a demand response mechanism, Energy Convers. Manag. 120 (y) (2016) 388–396.
[29] L. Valverde, F. Rosa, C. Bordons, J. Guerra, Energy management strategies in hydrogen smart-grids: a laboratory experience, Int. J. Hydrog. Energy 41 (ust(31)) (2016) 13715–13725.
[30] G. Cau, D. Cocco, M. Petrollese, S.K. Kær, C. Milan, Energy management strategy based on short-term generation scheduling for a renewable microgrid using a hydrogen storage system, Energy Convers. Manag. 87 (ember) (2014) 820–831.
[31] Y. Ben-Haim, Info-Gap Decision Theory: Decisions Under Severe Uncertainty, Elsevier, 2006.
[32] S. Nojavan, H. Ghesmati, K. Zare, Robust optimal offering strategy of large consumer using IGDT considering demand response programs, Electr. Power Syst. Res. 130 (uary) (2016) 46–58.
[33] S. Nojavan, H. Pashaei-Didani, K. Saberi, K. Zare, Risk assessment in a central concentrating solar power plant, Solar Energy 180 (ch) (2019) 293–300.
[34] J. Jannati, D. Nazarpour, Optimal energy management of the smart parking lot under demand response program in the presence of the electrolyser and fuel cell as hydrogen storage system, Energy Convers. Manag. 138 (il) (2017) 659–669.
[35] The GAMS Software Website, (2019).
[36] The GAMS Software Website, (2019).